

**Research paper****High Signal to Noise Ratio in Miniaturized Atomic Cells by Frequency Modulation Spectroscopy Method***A. Mirazei, M. Sotoudeh, M. Asadolahsalmanpour, M. Mosleh, S. M. Hamidi** *Magneto-Plasmonic Lab, Laser and Plasma Research Institute, Shahid Beheshti University, Tehran, Iran.**[*m_hamidi@sbu.ac.ir](mailto:m_hamidi@sbu.ac.ir)***Article info:****Article history:**

Received: 01/06/2025

Accepted: 12/06/2025

Keywords:

Atomic magnetometer, Rubidium microcell, Frequency modulation spectroscopy, Amplitude modulation spectroscopy, Magneto-plasmonics.

Abstract

Miniaturized atomic vapor cells are emerging as essential components in various applications such as brain signal tracking, nitrogen-vacancy center magnetometry, and electric and magnetic field sensing. However, achieving a high signal-to-noise ratio (SNR) in these compact systems remains a key challenge, which can be addressed using selective spectroscopic techniques.

In this study, we present a novel type of atomic vapor cell based on hot rubidium vapor, designed to enhance the spatial resolution of magnetometers. We also demonstrate the advantages of frequency modulation spectroscopy in improving spectral resolution. The cells are fabricated under a base pressure of 10^{-3} mbar and filled with nitrogen gas in a clean vacuum environment.

The integration of these miniaturized cells with spectroscopic techniques enables their use in laser feedback loops to lock onto specific atomic transitions. This approach provides new possibilities for next-generation quantum technologies, including quantum sensors, atomic clocks, and quantum computing systems.

1. Introduction

Spectroscopic methods based on hot alkali vapors have enabled a wide range of applications in the first generation of quantum metrology devices, such as atomic clocks [1–3], atomic filters [4–6], and atomic magnetometers [7–11]. The integration of optical phenomena, such as evanescent waves and plasmonic modes within nanostructured platforms, with hot atomic vapors has opened new avenues for designing

highly sensitive and high-resolution sensor heads [12,13].

Moreover, miniaturizing these atomic plasmonic cells to the nano- or microscale has been proposed as a way to enhance both sensitivity and spatial resolution by mitigating various broadening effects [14]. In addition to miniaturization, achieving a high signal-to-noise ratio (SNR) is crucial for improving sensitivity and spatial resolution. Measurement techniques that address this include pump-probe methods such as spin-exchange relaxation-free (SERF)



magnetometry [15], electromagnetically induced transparency (EIT) [16], and amplitude or frequency modulation spectroscopy (AMS/FMS) [17,18].

In this study, we investigate the optical transmission of a newly designed and fabricated rubidium (Rb) microcell using frequency modulation spectroscopy (FMS). We demonstrate that miniaturizing the hot vapor cell significantly reduces Doppler broadening in the Rb atomic transitions. Our findings also indicate that Rb microcells can enable precise measurement of atomic transition lines, which is critical for laser frequency locking in atomic sensors, as well as in highly sensitive biomedical recording systems such as magnetoencephalography (MEG) and magnetocardiography (MCG), which require detection of ultra-low magnetic fields.

2. Miniaturisation effect

The polarization induced by the dipole moments of gas atoms depends on the electric field and can be calculated using the atomic density matrix. The equation describing the dipole moments relies on boundary conditions defined by the excitation processes of near-surface atoms. In the regime where the mean free path of gas atoms exceeds the thickness of the boundary layer where the optical response is formed, separate boundary conditions must be applied for atoms moving toward and away from the surface. The most realistic and simple assumption is that atoms reaching the surface are absorbed and then re-emitted (reflected) with zero polarization.

The dipole moments and the atomic susceptibility in these two directions can be written as follows:

$$\begin{aligned}\mu_-(r, t) &\approx \frac{ie^2 f}{2m_e \omega_0} \frac{1}{\gamma - i(\Delta - k_i \cdot v)} E_{t0} e^{ik_i \cdot r} e^{-i\omega t} \\ \chi_-(z) &= n \int_{v_z \leq 0} f_M(v) \frac{ie^2 f}{2m_e \omega_0} \frac{1}{\gamma - i(\Delta - k_i \cdot v)} dv \\ \mu_+(r, t) &\approx \frac{ie^2 f}{2m_e \omega_0} \frac{1}{\gamma - i(\Delta - k_i \cdot v)} \\ &\left\{ 1 - \exp \left[-\frac{\gamma - i(\Delta - k_i \cdot v)}{v_z} z \right] \right\} E_{t0} e^{ik_i \cdot r} e^{-i\omega t}\end{aligned}$$

$$\begin{aligned}\chi_+(z) &= n \int_{v_z > 0} f_M(v) \frac{ie^2 f}{2m_e \omega_0} \frac{1}{\gamma - i(\Delta - k_i \cdot v)} \\ &\left\{ 1 - \exp \left[-\frac{\gamma - i(\Delta - k_i \cdot v)}{v_z} z \right] \right\} dv\end{aligned}$$

Where $\alpha(\omega; v)$ denoting the atomic polarizability as a function of Doppler broadening, here we want to define Variable

$$\text{parameters such as } f_M(v) = \frac{1}{\pi^{3/2} v_t^3} \exp \left(-\frac{v^2}{v_t^2} \right)$$

where f_M is Maxwellian velocity distribution function, v_t is the most probable thermal velocity, $k_i \cdot v$ is term of Doppler broadening where v is atom velocity and k_i is wave vector, n is the number density of the gas atom.

It is observed that the spatial dependence of the contribution from arriving atoms closely follows the spatial variation of the external field. In contrast, the contribution from scattered atoms does not exhibit the same behavior due to the presence of an exponential term in the expression (within the curly brackets). Additionally, the Doppler broadening term appears explicitly in the atomic polarizability expression, where it plays a significant role in determining the induced dipole moments and the overall atomic susceptibility.

As a second step to enhance the signal-to-noise ratio, we employ high-precision modulation techniques such as amplitude modulation (AM) and frequency modulation (FM) spectroscopy.

When the laser is tuned through the absorption spectrum, the difference

$$\Delta p_T = p_T \left(\omega_L - \frac{\Delta \omega_L}{2} \right) - p_T \left(\omega_L + \frac{\Delta \omega_L}{2} \right) \quad \text{is}$$

detected with a lock-in amplifier which tuned to the modulation frequency, Ω . In this method, if

the modulation sweep $\Delta \omega_L$ is small enough, the first sentence corresponds to the first derivative of the absorption spectrum is dominant in Taylor expansion [20]:

$$\Delta p_T(\omega) = \frac{dp_T}{d\omega} \Delta \omega_L + \frac{1}{2!} \frac{d^2 p_T}{d\omega^2} \Delta \omega_L^2 + \dots$$

If the laser frequency $\omega_L(t) = \omega_0 + a \sin \Omega t$ is sinusoidally modulated at the modulation frequency, the Taylor expansion will be obtained as follows:

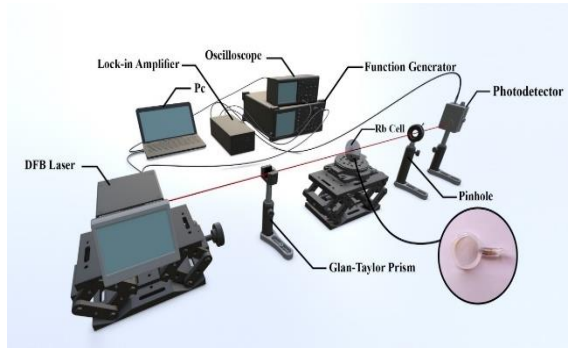
$$p_T(\omega) = p_T(\omega_0) + \sum_n \frac{a^n}{n!} \sin^n \Omega t \left(\frac{d^n p_T}{d\omega^n} \right)_{\omega_0}$$

The main signal of absorption spectrum, $\alpha(\omega)$, and the first derivative of that are shown in the Figure 1(d) which confirms that the size of FWHM decreases by $\gamma/\sqrt{3}$ and thus the spectral resolution increases at each order of derivation [20].

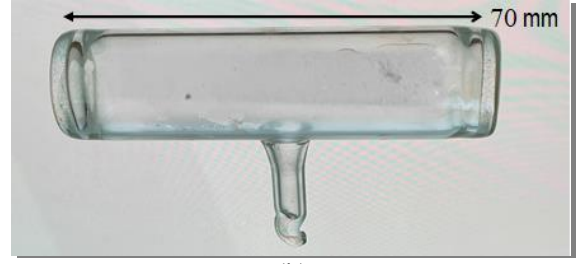
3. Experimental Method

To investigate the effect of cell miniaturization on the spectroscopic properties of rubidium (Rb) vapor, three borosilicate glass cells of different sizes were prepared: a reference cell with dimensions of 25 mm \times 70 mm, a microcell in the form of a 700 μ m diameter glass strip, and a circular cell, each designed and fabricated as reference and miniaturized versions, respectively. The cells were fabricated using standard glassblowing techniques. To prevent unwanted chemical reactions between the highly reactive rubidium metal and contaminants, all cells were thoroughly cleaned and dried under high vacuum and elevated temperature conditions [19]. A mixture of rubidium vapor and argon buffer gas was then introduced into each cell under vacuum. The cells were subsequently sealed using a fire torch. The purpose of the buffer gas is to reduce both collisional and Doppler broadening by shortening the mean free path of the Rb atoms.

Figures 1a, 1b, and 1c illustrate the experimental setup, the fabricated reference cell, and the miniaturized microcell, respectively.



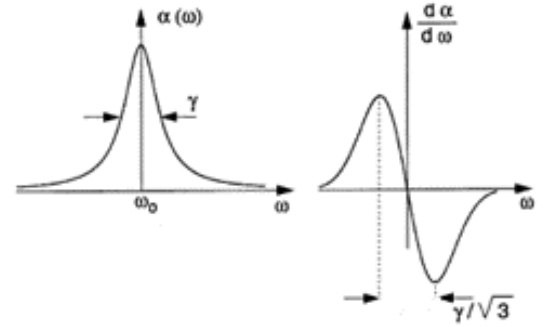
(a)



(b)



(c)



(d)

Figure 1: (a) Schematic diagram of the experimental setup, with the circular cell shown in the inset; (b) reference cell with dimensions of 25 mm \times 70 mm; (c) miniaturized rubidium vapor cell with dimensions of 5 cm \times 700 μ m; and (d) absorption spectrum and its first derivative obtained from reference [20].

In this experimental setup, 795 nm laser light from a distributed feedback (DFB) laser is modulated in amplitude or frequency. After passing through a Glan-Taylor prism, the vapor cells, and a pinhole, the modulated light reaches the detector. The combination of modulation techniques and the miniaturization of the vapor cells is used to eliminate Doppler broadening in atomic spectra. The optical properties of rubidium (Rb) vapor cells were investigated using amplitude modulation spectroscopy (AMS) and frequency modulation spectroscopy

(FMS), as shown in Figure 2(a). In AMS, the laser light is modulated by an electro-optical modulator, and the intensity of the modulated light is measured using a lock-in amplifier (LIA). Any change in the modulated light intensity caused by absorption in the Rb vapor is accurately detected. The purpose of modulation in AMS is to eliminate intensity fluctuations caused by external factors.

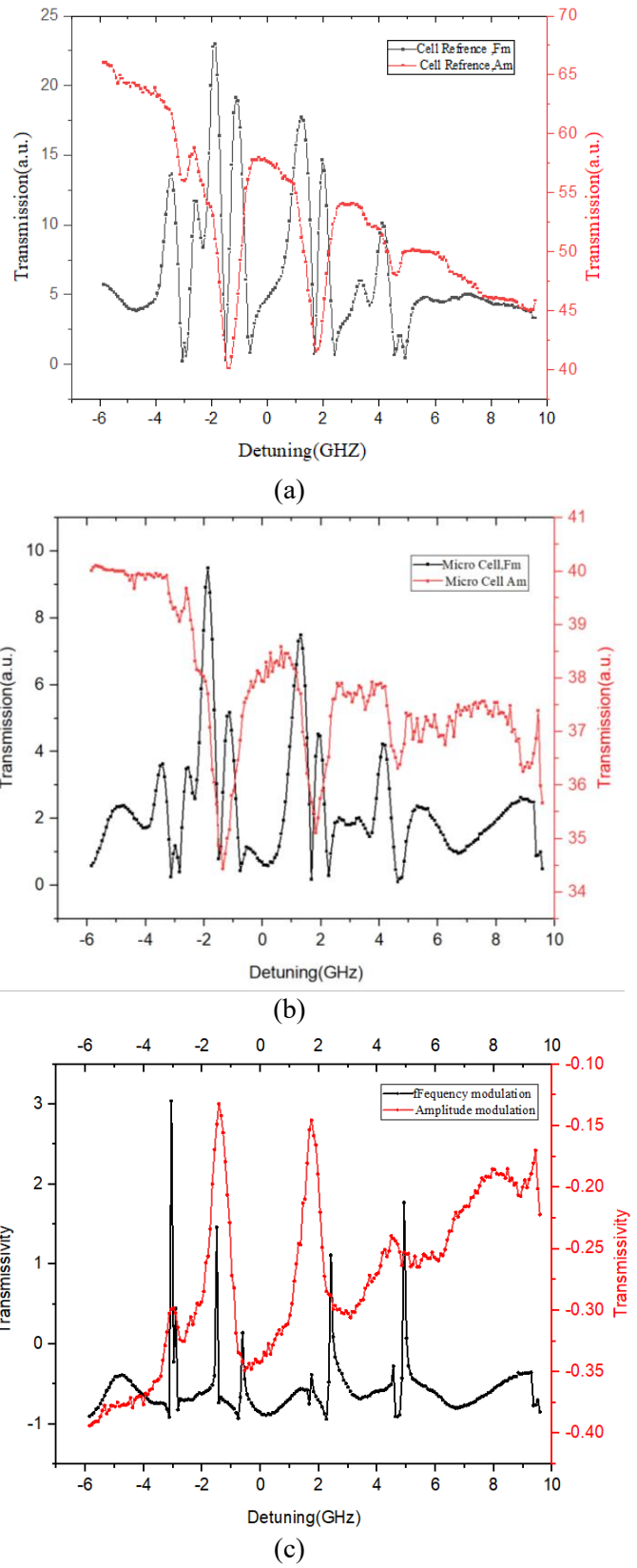
In FMS, the laser frequency is modulated around a set point, which is also swept across the absorption frequency range.

Absorption by Rb atoms modulates the laser intensity, and after demodulation by the LIA, the derivative of the absorption lines is obtained. At the initial stage, reducing the size of the vapor cells enhances spectral resolution by spatially confining the vapor to a cell thickness comparable to the incident wavelength. This confinement creates a transient state of light-atom interactions, allowing slower atoms to contribute significantly to the signal.

Vartanian developed the theory of selective transmission and reflection from a thin vapor layer confined between two parallel walls, showing that Doppler-free resonance depends on the vapor layer thickness. To excite the vapor with a continuous wave plane wave, the transition field at the solid-vacuum interface is described by Fresnel formulas inside the cell [21,22].

4. Results and discussion:

Figure 2 compares the absorption spectra of rubidium vapor obtained using amplitude modulation (AM) and frequency modulation (FM) spectroscopy for the reference cell. AM spectroscopy provides a direct measurement of the atomic absorption lines, while the FM spectroscopy output, due to its derivative nature, highlights the detuning more precisely. The center of each dispersive-shaped signal in FM spectroscopy corresponds to the exact frequency of the atomic transition.



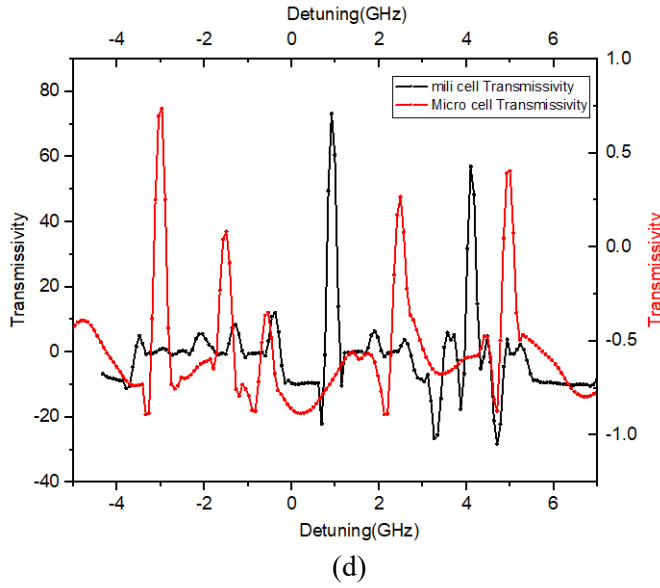


Figure 2:(a) Transmission data from the reference rubidium vapor cell using amplitude modulation (measured at 52°C) and frequency modulation (measured at room temperature). (b) Transmission data from the microcell obtained via amplitude and frequency modulation techniques. (c) Transmissivity of the microcell analyzed by both amplitude and frequency modulation methods. (d) Comparison of the transmissivity spectra between microcell and millimeter-scale (reference) cell.

Comparison between AM and FM spectroscopy results shows that frequency modulation spectroscopy (FMS) reveals more absorption lines than amplitude modulation spectroscopy (AMS). Therefore, FMS offers significantly higher spectral resolution. Another well-known advantage of FMS is its higher sensitivity and larger signal-to-noise ratio (SNR), which enables accurate measurements at lower rubidium atom densities and thus at lower cell temperatures compared to AMS. The corresponding results of AMS and FMS for the microcell at the same temperature are shown in Figure 2(b).

In microcells, the primary mechanism for Doppler broadening suppression is related to the polarization dynamics of the transiting atoms, which is often neglected in conventional models.

The overlap of contributions from atoms oscillating between opposite walls leads to a periodic dependence of the spectral line shape on the cell thickness, thereby further enhancing Doppler-free effects [22]. Wall collisions allow atoms to oscillate freely at their natural frequency. In cells with thickness smaller than the mean free path of atoms, these atoms do not have sufficient time to respond to the external optical field, and their polarization remains unchanged after surface collisions. As the cell thickness increases, atoms have enough time to adapt to the optical field before colliding with the walls, leading to polarization changes and consequently Doppler broadening in the spectrum.

Similar to the reference cell, FMS measurements in the microcell demonstrate a higher spectral resolution than AMS. Comparing FMS results for reference and micro cell does not show so much difference in first sight, but to show differences more precisely way we calculate transmissivity as $\frac{\Delta T_s}{T_s^0}$, in which, $\Delta T_s = T - T_0$.

Result of calculation of transmissivity for absorption spectrums of AMS and FMS for reference and microcell show in Figs. 2(c) and (d). One can see Doppler free absorption from FMS signal of micro cell as transition lines of rubidium cells. The practical implications of miniaturizing rubidium vapor cells and utilizing frequency modulation spectroscopy are significant for the advancement of quantum sensing technologies. Enhanced spectral resolution and sensitivity enable the development of highly accurate atomic magnetometers and clocks with reduced size and power consumption.

5. Conclusion

Our results demonstrate that reducing the dimensions of the rubidium vapor cell—from reference scale to millimeter and micro scales—leads to increased sensitivity, due to the improved accuracy in resolving atomic transitions. This enhancement, combined with the improved spatial resolution achieved through miniaturization and the use of frequency

modulation spectroscopy, strongly supports the development of compact, high-performance atomic-based devices. These advantages motivate further research and innovation toward the miniaturization of next-generation quantum sensors and related technologies.

Declaration:

Ethics approval and consent to participate:

Not applicable.

Consent for publication:

Not applicable.

Availability of data and materials:

Data available from the corresponding author by request.

Competing interests:

There is no any conflict of interest.

Funding:

There is no any finding.

Authors' contributions:

S. M. Hamidi supervise all of the work and writing process, A. Mirzaei, and M. Asadollahsalmanpour and M. Sotoudeh measure all of samples and M. Mosleh fabricate the cells and align measurement setup.

References

1. P. D. D. Schwindt, S. Knappe, V. Shah, L. Hollberg, J. Kitching, L.-A. Liew, and J. Moreland, Chip-scale atomic magnetometer. *Applied Physics Letters*, 85(26), 6409-6411, (2004).
2. S. Knappe, P. D. D. Schwindt, V. Shah, L. Hollberg, J. Kitching, L. Liew, and J. Moreland, A chip-scale atomic clock based on ^{87}Rb with improved frequency stability, *Opt. Express* **13**, 1249 (2005).
3. M. M. Boyd, A. D. Ludlow, S. Blatt, S. M. Foreman, T. Ido, T. Zelevinsky, and J. Ye, ^{87}Sr Lattice Clock with Inaccuracy below 10^{-15} , *Phys. Rev. Lett.* **98**, 083002 (2007).
4. M. A. Zentile, J. Keaveney, L. Weller, D. J. Whiting, C. S. Adams, and I. G. Hughes, ElecSus: A program to calculate the electric susceptibility of an atomic ensemble, *Comput. Phys. Commun.* **189**, 162 (2015).
5. Kiefer, W., Löw, R., Wrachtrup, J., [Gerhardt](#), I. Na-Faraday rotation filtering: The optimal point. *Sci Rep* **4**, 6552 (2014).
6. J. Keaveney, S. A. Wrathmall, C. S. Adams, and I. G. Hughes, Optimized ultra-narrow atomic bandpass filters via magneto-optic rotation in an unconstrained geometry, *Opt. Lett.* **43**, 4272 (2018).
7. J. Keaveney, C. S. Adams, and I. G. Hughes, Elecsus: Extension to arbitrary geometry magneto-optics, *Comput. Phys. Commun.* **224**, 311 (2018).
8. G. Bison, R. Wynands, and A. Weis, Dynamical mapping of the human cardiomagnetic field with a room-temperature, laser-optical sensor, *Opt. Express* **11**, 904 (2003).
9. P. D. D. Schwindt, S. Knappe, V. Shah, L. Hollberg, J. Kitching, L.-A. Liew, and J. Moreland, Chip-scale atomic magnetometer, *Appl. Phys. Lett.* **85**, 6409 (2004).
10. M. V. Balabas, D. Budker, J. Kitching, P. D. D. Schwindt, and J. E. Stalnaker, Magnetometry with millimeter-scale antirelaxation-coated alkali-metal vapor cells, *J. Opt. Soc. Am. B* **23**, 1001 (2006).
11. D. Budker and M. Romalis, Optical magnetometry, *Nat. Phys.* **3**, 227 (2007).
12. G. Bison, N. Castagna, A. Hofer, P. Knowles, J. L. Schenker, M. Kasprzak, H. Saudan, and A. Weis, A room temperature 19-channel magnetic field mapping device for cardiac signals, *Appl. Phys. Lett.* **95**, 173701 (2009).
13. R. Wyllie, M. Kauer, R. T. Wakai, and T. G. Walker, Optical magnetometer array for fetal magnetocardiography, *Opt. Lett.* **37**, 2247 (2012).
14. T. F. Cutler, W. J. Hamlyn, J. Renger, K. A. Whittaker, D. Pizzey, I. G. Hughes, V. Sandoghdar, C. S. Adams, "Nanostructured Alkali-Metal Vapor Cells", *Physical Review Applied*, **14**, 034054 (2020).

15. W. E. Bell and A. L. Bloom, Optically Driven Spin Precession, *Phys. Rev. Lett.* **6** (1961) 280-281.
16. E. Klinger, H. Azizbekyan, A. Sargsyan, C. Leroy, D. Sarkisyan, and A. Papoyan, Proof of the feasibility of a nanocell-based wide-range optical magnetometer, *Appl. Opt.* **59**, 2231 (2020).
17. G. C. Bjorklund, Frequency-modulation spectroscopy: a new method for measuring weak absorptions and dispersions. *Optics letters*, **5**(1), 15-17, (1980).
18. D. G. Cameron, D. J. Moffatt, A generalized approach to derivative spectroscopy. *Applied spectroscopy*, **41**(4), 539-544, (1987).
19. M. Mosleh., M. Ranjbaran., S. M. Hamidi . Trace of evanescent wave polarization by atomic vapor spectroscopy. *Scientific Reports*, **11**(1), 1-9. (2021).
20. W. Demtroder. *Laser spectroscopy: vol.2: experimental techniques*. Springer Science & Business Media, (2008)
21. A. V. Ermolaev, T. A. Vartanyan. "Rigorous theory of thin-vapor-layer linear optical properties: The case of specular reflection of atoms colliding with the walls", *Physical Review A*, Vol 101, No 5 ,pp.05385-05393, (2020).
22. V. G. Bordo, H. G. Rubahn. *Optics and spectroscopy at surfaces and interfaces*. John Wiley & Sons (2008).